*Proc. Natl. Acad. Sci. USA*
Vol. 95, pp. 6118–6121, May 1998
Biophysics

# Huntingtin aggregation monitored by dynamic light scattering

**(Huntington's disease/fibrillogenesis)**

YANNIS GEORGALIS*, E. B. STARIKOV†, BIRGIT HOLLENBACH†, RUDI LURZ†, EBERHARD SCHERZINGER†, WOLFRAM SAENGER*, HANS LEHRACH†, AND ERICH E. WANKER†‡

†Max-Planck-Institut für Molekulare Genetik, Ihnestr. 73, D-14195 Berlin, Germany; and *Institut für Kristallographie, Freie Universität Berlin, Takustr. 6, D-14195 Berlin, Germany

*Communicated by Max F. Perutz, Medical Research Council, Cambridge, United Kingdom, March 18, 1998 (received for review November 27, 1997)*

**ABSTRACT** **An initial stage of fibrillogenesis in solutions of glutathione *S*-transferase-huntingtin (GST-HD) fusion proteins has been studied by using dynamic light scattering. Two GST-HD systems with poly-L-glutamine (polyGln) extensions of different lengths (20 and 51 residues) have been examined. For both systems, kinetics of z-average translation diffusion coefficients ($D_{app}$) and their angular dependence have been obtained. Our data reveal that aggregation does occur in both GST-HD51 and GST-HD20 solutions, but that it is much more pronounced in the former. Thus, our approach provides a powerful tool for the quantitative assay of GST-HD fibrillogenesis *in vitro*.**

Huntington's disease (HD) is an autosomal dominant progressive neurodegenerative disorder manifesting itself as personality changes, motor impairment, and subcortical dementia (1). On the molecular level, it is caused by a CAG/poly-L-glutamine (polyGln) repeat expansion in the first exon of a gene encoding a large protein of unknown function, so-called huntingtin (2). These repeats range from 6 to 39 on chromosomes of unaffected individuals and from 36 to 180 on HD chromosomes (3). The majority of adult HD onset cases contain 40- to 55-unit-long CAG repeats, whereas CAG expansions of more than 70 units invariably cause the juvenile form of the disease (4).

The mechanism by which an elongated polyGln sequence causes neurodegeneration within the frame of HD is largely unknown. It is believed that the presence of elongated polyGln causes a toxic gain of function in huntingtin (5). Physically, this condition should correspond to the onset of abnormal protein–protein interactions, which lead to an avalanche of protein aggregation and finally to cell death. One of the hypotheses concerning the molecular mechanism of HD is connected with the capability of polyGln sequences to act as "polar zippers" (6, 7): polyGlns form pleated sheets of $\beta$-strands held together by hydrogen bonds between their amides, raising a possibility of polyGln self-aggregation.

A major research effort in trying to clarify the molecular mechanisms underlying HD is directed toward constructing *in vitro* model systems capable of mimicking the HD events *in vivo*. To this end, the use of exon 1 of the HD gene with normal and expanded CAG repeats for the production of glutathione *S*-transferase (GST)-HD fusion proteins in *Escherichia coli* has been reported very recently (8). Site-specific proteolysis of a GST-HD51 fusion protein with a polyGln expansion in the pathological range (51 glutamines) resulted in the formation of high molecular weight protein aggregates with a fibrillar or ribbon-like morphology. These filaments, which were not produced by proteolysis of shorter fusion proteins (20 or 30 glutamine units), were similar to scrapie prions and $\beta$-protein fibrils in Alzheimer's disease. They also resembled the fibrillar structures detected by electron microscopy within the neuronal intranuclear inclusions of mice transgenic for the HD mutation (9). What remains largely unknown, however, is the detailed molecular structure and physico-chemical mechanisms of formation of the GST-HD filaments.

The recent success in constructing an *in vitro* system for modeling HD at the molecular level (8) raises inviting prospects for finding a remedy for HD. To cope with this formidable task, some physico-chemical technique (or, possibly, a combination of them) is clearly necessary to reliably characterize and monitor the process of GST-HD aggregation in the presence of its potential inhibitors. Thus, the aim of this study was to establish a physico-chemical method with which one could analyze the process of the GST-HD filament formation after site-specific proteolytic cleavage of the fusion protein.

Here the well-known method of dynamic light scattering (DLS) (10–12) was applied, because, in contrast to most other methods, the sample could be examined in a noninvasive manner. Moreover, this method has been successfully applied for studying the nucleation and growth of Alzheimer's $\beta$-amyloid fibrils (13–17). In the present study, we focus on the initial state of the GST-HD20 and GST-HD51 (8) preparations. According to our view, it is important to understand the initial aggregation states because they greatly influence all other solution properties. Our results show that DLS is well suited to study the dynamics of huntingtin aggregation, and the data, which are in qualitative agreement with our previous biochemical and electron-microscopic studies (8), allow us to gain some additional insight into the kinetics of GST-HD fibrillogenesis *in vitro*.

## MATERIALS AND METHODS

**Protein Preparations.** In this work, GST-HD20 and GST-HD51, i.e., fusion proteins containing 20- and 51-residue-long polyGln extensions were used. Expression and purification of the GST fusion proteins, their site-specific cleavage with trypsin, SDS/PAGE, Western blotting, and electron-microscopic analysis were carried out as described in ref. 8.

**Light Scattering.** Laser light scattered by particles undergoing Brownian motion is detected in the direction of the scattering angle $\theta$. The resulting spectrum of intensity fluctuations contains information on the relaxation times typifying the translational, rotational, or internal motions of the particles, depending on their size and shape, and on the nature of their interactions. The spatial resolution in such experiments is defined by the wavevector of the scattered light whose magnitude $q$ is given by Bragg's formula: $q = (4\pi n/\lambda)\sin(\theta/2)$ where $\lambda$ denotes the wavelength of the scattered light *in vacuo* and $n$ is the refractive index of the solvent. Ideally, for

The publication costs of this article were defrayed in part by page charge payment. This article must therefore be hereby marked "*advertisement*" in accordance with 18 U.S.C. §1734 solely to indicate this fact.

© 1998 by The National Academy of Sciences 0027-8424/98/956118-4$2.00/0
PNAS is available online at http://www.pnas.org.

Abbreviations: GST-HD, glutathione *S*-transferase-huntingtin; DLS, dynamic light scattering; polyGln, poly-L-glutamine; HD, Huntington's disease.

‡To whom reprint requests should be addressed.

noninteracting spherical particles, DLS directly delivers the z-average translational diffusion coefficient $D_{app}$ (18), which is associated with the hydrodynamic radius ($R_h$) of the particles as $R_h = k_B T/6\,\pi\,\eta\,D_{app}$. Here, $k_B T$ denotes the thermal energy and $\eta$ the viscosity of the solvent. More complex treatments must be involved if particles with dimensions comparable to the wavelength of light are examined or when the particles interact with each other.

The present work is confined only to characterizing the initial phase of the GST-HD20 and GST-HD51 aggregation in aqueous solutions after a mild trypsin treatment, as documented by the time dependence of the apparent diffusion coefficients $D_{app}$ (which, however, typify only average solution properties).

Light scattering experiments were conducted with an ALV/SP-86 spectrogoniometer (ALV, Langen, Germany) using a Spectraphysics (Stabilite 2017) Ar+ laser (1.8 W output power at a wavelength of 488 nm). After amplification and discrimination, signals are directed to the ALV-5000/E-FAST multitau-multibit digital correlator boards and spectra are recorded on 255 channels, quasi-logarithmically spaced in time. Angular dependence experiments covered the range between 15° and 150°, corresponding to scattering vectors between $4.40 \times 10^{-3}$ and $3.32 \times 10^{-2}$ $nm^{-1}$. For a typical experiment the correlation function spans theoretically the range between 12.5 ns and 60 s, and correlograms were acquired for times varying between 30 and 60 s. Apparent diffusion coefficients were determined with the method of cumulants (19) by fitting variable degree polynomials to the first 50 channels of each correlogram as previously described (20). The quoted apparent diffusion coefficients were corrected to standard conditions, water and 293.2°K.

Fifty spectra were collected at 293.2°K to get estimates of the diffusion coefficient and relative polydispersity of the solutions before trypsin treatment. On completion of these measurements 50 $\mu$l of 0.25 mg/ml of trypsin and 45 $\mu$l of 50 mM $CaCl_2$ were added to 1 ml of GST-HD solution of concentration 1 mg/ml [enzyme/substrate ratio of 1:80 (wt/wt)]. These operations were performed under a clean bench to avoid residual dust contamination. Finally, temperature was slowly brought up to 310.2°K, and then spectra were collected for 4 hr, until the solutions had reached their quasi-stationary state. The angular dependence of the diffusion coefficient was determined the next day at 310.2°K.

## RESULTS AND DISCUSSION

The apparent diffusion coefficient of the intact protein (before trypsin treatment) was determined by averaging the results of 50 spectra. We have obtained values of $(1.07 \pm 0.02)$ and $(1.17 \pm 0.02) \times 10^{-7}$ $cm^2\ s^{-1}$, for the GST-HD20 and GST-HD51 preparations, respectively. The normalized second cumulant was equal to $(0.20 \pm 0.04)$ and $(0.30 \pm 0.03)$, respectively. At 293.2°K trypsin action is extremely slow and allows recording a number of correlograms under virtually nonaggregation conditions. For the GST-HD20 sample there were no appreciable differences detected from the above-quoted estimates on addition of trypsin and $CaCl_2$. Slightly smaller values for $D_{app}$, approximately by 10–20%, were obtained for the GST-HD51 preparation, which is indicative of some trypsin action already at 293.2°K.

A schematic representation of the primary structure of the polyGln-containing fusion proteins GST-HD20 und GST-HD51 and the relevant trypsin cleavage sites within the fusion proteins are shown in Fig. 1*A*. The protease trypsin cleaves off the GST-tag together with an additional 15 amino acids from the N terminus and a single proline from the C terminus of the HD exon 1 proteins, but leaves the polyGln repeat intact (8). After addition of trypsin to the fusion proteins GST-HD20 and GST-HD51 samples were taken at different times and analyzed by SDS/PAGE and immunoblotting using the HD1 antibody (8). Fig. 1*B* shows that proteolytic cleavage of both fusion proteins has occurred within 30 min at 37°C. The cleavage of GST-HD20 with an apparent molecular mass of 40 kDa resulted in the formation of a product migrating at about 30 kDa, whereas the cleavage of GST-HD51 with an apparent molecular mass of about 50 kDa resulted in the formation of two higher molecular mass bands migrating at about 60 and 170 kDa, and an additional immunoreactive band remaining at the top of the gel. This band corresponds to the aggregated HD exon 1 protein (8). Thus, our data enable us to conclude that there is no significant difference between GST-HD20 and GST-HD51 sensitivity to tryptic cleavage or in their cleavage kinetics.

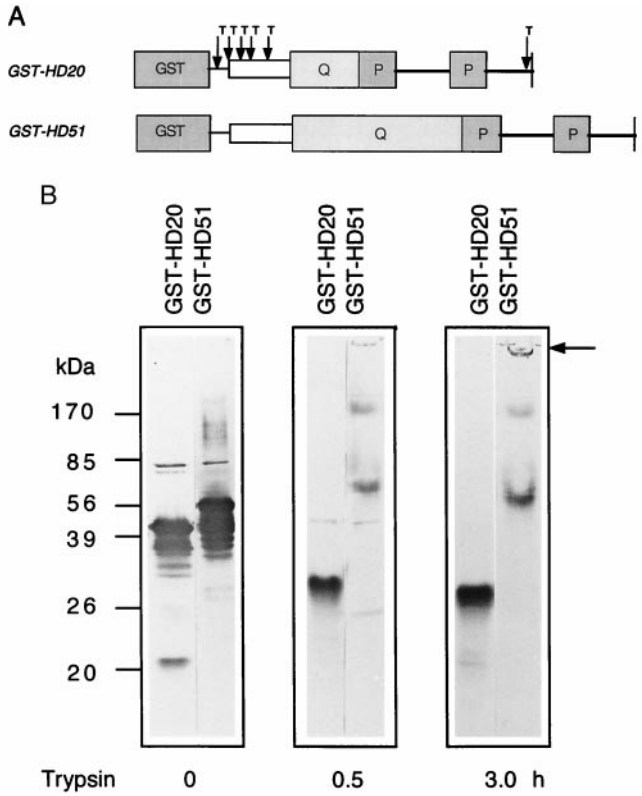


FIG. 1. (*A*) Schematic representation of primary structure of GST-HD fusion proteins. The amino acid sequence corresponding to exon 1 of huntingtin is boxed. Q and P stand for polyglutamine and polyproline extensions, respectively. Arrows and T indicate cleavage sites for trypsin. (*B*) Site-specific proteolysis of GST-HD fusion proteins with trypsin. Tryptic digestions were performed at 37°C for the indicated times. Undigested and trypsin-digested proteins were subjected to 12.5% SDS/PAGE, blotted onto nitrocellulose membranes, and probed with the anti-huntingtin antibody HD1. Arrow marks the origin of electrophoresis.

Fig. 2*a* displays the $D_{app}(t)$ for GST-HD20 and GST-HD51 as a function of aggregation time. Obviously, the 20-mer and 50-mer aggregate to a different extent, so that $D_{app}(t)$ follows dissimilar kinetics for each polyGln extension chain length. The terminal $D_{app}(t)$ for GST-HD51 is about five times lower than that detected for GST-HD20. Even more persuasive in this respect appears the behavior of the normalized second cumulant, which is used as a qualitative measure of the solution polydispersity (aggregation is nonspecific, thus giving rise to a high polydispersity), cf. Fig. 2*b*. This figure shows the terminal polydispersity of GST-HD51 to be approximately two orders of magnitude higher than that of GST-HD20. This difference should be indicative of a drastically increased cohesion within GST-HD51 aggregates, as compared with GST-HD20.

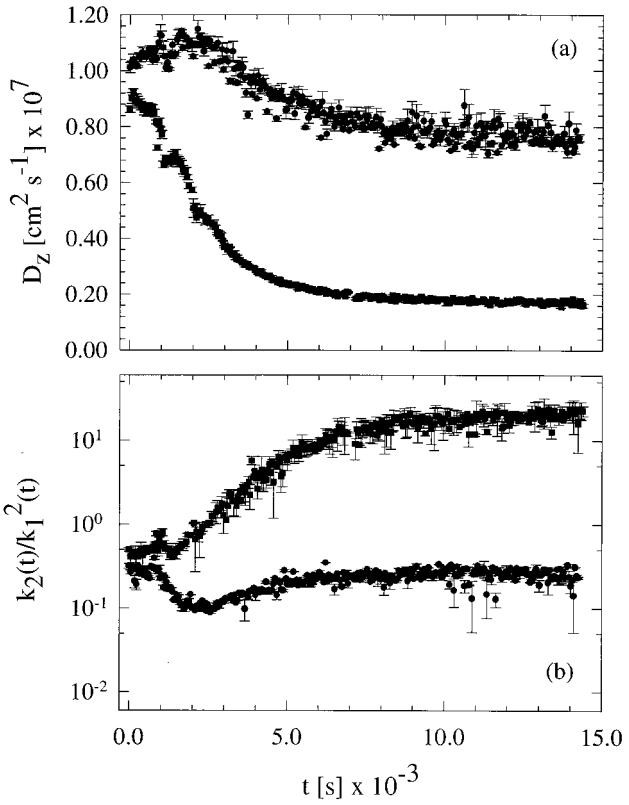


FIG. 2. (*a*) Apparent diffusion coefficient $D_{app}(t)$ plotted as function of time for selected fusion protein preparations GST-HD20 (●) and GST-HD51 (■). Measurements were conducted at a fixed scattering angle, 45°. (*b*) Normalized second cumulant of GST-HD20 (●) and GST-HD51 (■) as a function of time. Note that the 5-fold drop of the apparent diffusion coefficient is accompanied by a 100-fold increment of the normalized second cumulant, which can be understood as a drastic increment of the solution polydispersity.

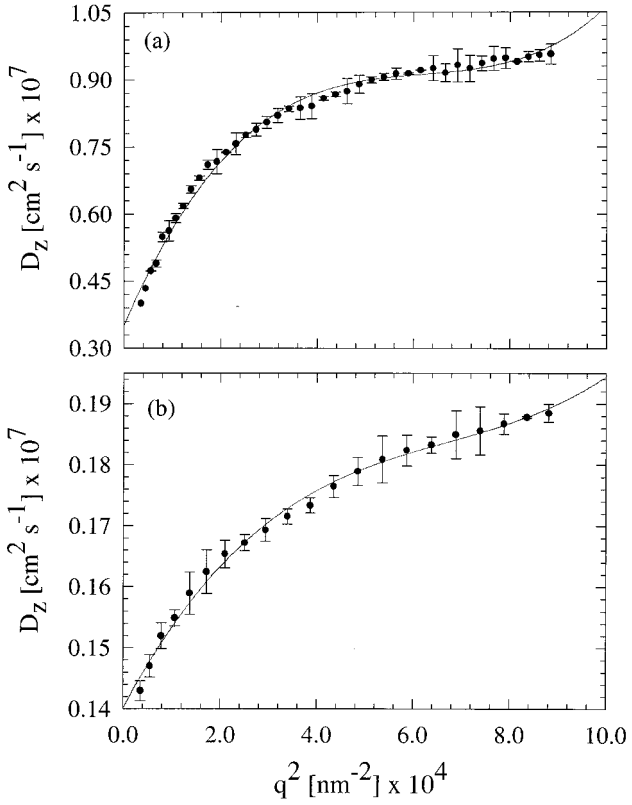


FIG. 3. Angular dependence of the z-average diffusion coefficient of the (*a*) GST-HD20 and (*b*) GST-HD51 protein preparations. SDs were estimated from an average of three experiments conducted 18 hr after collecting the time-resolved results shown in Fig. 2. Note that the $q^2$ dependence of $D_{app}$ for both samples deviates appreciably from linearity. Further, the GST-HD20 sample exhibits roughly a two times higher limiting $D_{app}(q)$ value than the GST-HD51 one.

Further, the diffusion coefficient angular dependence for the trypsin-treated GST-HD20 and GST-HD51 samples was examined at 310.2°K after 18 hr, on completion of the kinetic experiments. For spherical particles, this dependence is expected to exhibit a linear $q^2$ scaling behavior. In contrast, pronounced deviations from linearity, when plotting $D_{app}(q)$ versus $q^2$, were observed for both of the samples (cf. Fig. 3). This behavior corroborates the formation of fibrillar structures in solutions as already shown by electron microscopy (cf. ref. 8 and Fig. 4). Interestingly, our DLS data allow us to anticipate some kind of aggregation even in the GST-HD20 samples, although no fibrillar structures have been detected by electron microscopy (cf. Fig. 4 and ref. 8). In this context, it should be noted that fibrillar structures are not trivial to study by light scattering even in well-behaved stationary solutions (21). Specifically, the behavior of fibrils should be strongly dependent on the interaction potential between the fibrils, on their flexibility and mean size polydispersity (22–26). To clarify the significance of these factors for the GST-HD systems in question, further protracted and systematic studies will be required.

Although the DLS data presented above do not allow us to discuss the mechanisms of GST-HD aggregation in detail, they undoubtedly lend support to the relevant mechanistic proposal we put forward very recently (8). Besides, it should be noted that the whole process of GST-HD aggregation is essentially reminiscent of the amyloid β-protein fibril formation (13–17), especially if we recall the striking visual similarity between the fibrils in Alzheimer's disease (27, 28) and those in HD and GST-HD (8, 9). Regrettably, this parallel does not help us to immediately gain a deeper insight into the GST-HD fibrillogenesis mechanism, because for the present there is no general agreement on the details of amyloid β-protein and scrapie aggregation pathways (e.g., ref. 27). Nevertheless, in HD polyGln extensions (*homo*polypeptides, unlike in Alzheimer's disease and scrapie) are known to be primarily responsible for the protein aggregation (6, 7). This fact appreciably facilitates any *a priori* modeling of GST-HD fibrillogenesis, as compared with that of amyloid β-proteins and prions.

Thus, if one adopts the model of ref. 8 arguing that the GST-HD fibrillogenesis is caused by a self-aggregation of polyGln extensions as "polar zippers" (6, 7), the prerequisite for the huntingtin nucleation could thermodynamically be thought of as a predominance of the cohesive forces between the polyGln extensions (enthalpy) over the Brownian motion of huntingtin molecules as a whole (entropy). Moreover, the inter-protein cohesive forces could noticeably increase only if the polyGln structural ordering (β-pleated sheet formation) is thermodynamically favorable (6, 7). Indeed, our estimations using a simple molecular-thermodynamical model (based on the ideas of M.F. Perutz, refs. 6 and 7) show that β-hairpin formation in aqueous solutions of polyGln chains becomes thermodynamically favorable when the chain length exceeds 40 residues, in striking accordance with the molecular-biological results on HD (3, 4, 9) (to be reported in detail elsewhere). A pronounced quantitative difference between the DLS results revealed here for the GST-HD20 and GST-HD51 proteins (cf. Figs. 2 and 3) supports the above theses.

To sum up, the present study shows that GST-HD fusion proteins with varying polyGln sequences provide a useful model system for additional studies on the mechanisms of

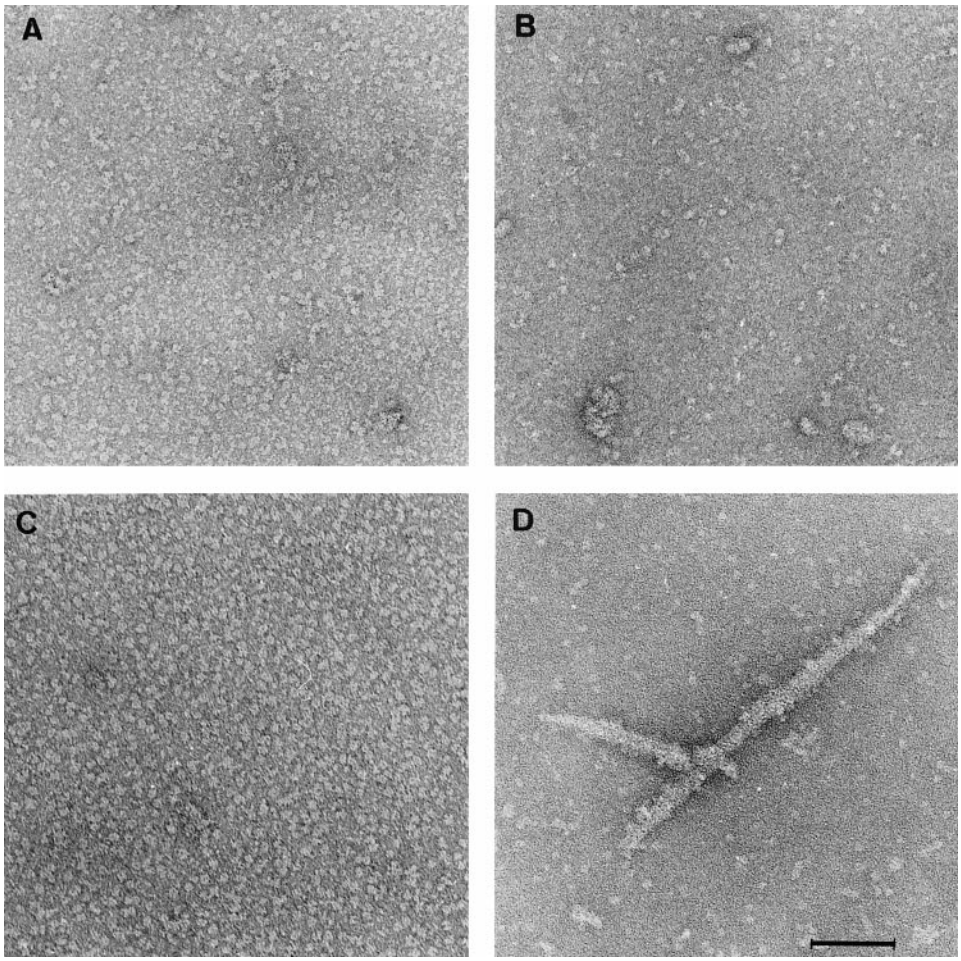


FIG. 4. Electron micrographs of GST-HD20 (*A* and *B*) and GST-HD51 (*C* and *D*) proteins before (*A* and *C*) and after (*B* and *D*) treatment with trypsin. Samples were negatively stained with 1% uranyl acetate. (Scale bar = 100 nm.)

huntingtin aggregation, and that the DLS method is a valuable tool in carrying out such studies. Detailed biochemical and biophysical investigations on the fibrillogenesis of GST-HD proteins with polyGln extensions consisting of 37–45 Gln residues are in progress in our laboratory, and the results will be communicated elsewhere.

Financial support to Y.G. from the Deutsche Forschungsgemeinschaft (Sa 196/26–1) is acknowledged. E.B.S. is greatly indebted to Max-Planck-Institute for Molecular Genetics, Berlin for financial support. E.E.W. wishes to acknowledge the financial support from Deutsche Forschungsgemeinschaft and grant from the European Union.

1. Harper, P. S., ed. (1991) *Huntington Disease* (Saunders, London), 22nd Ed.
2. The Huntington Disease Collaborative Research Group (1993) *Cell* **72,** 971–983.
3. Sathasivam, K., Amaechi, I., Mangiarini, L. & Bates, G. P. (1997) *Hum. Genet.* **99,** 692–695.
4. Rubinsztein, D. C., Leggo, J., Coles, R., Almquist, E., Biancalana, V., Cassiman, J. J., Chotai, K., Connarty, M., Crauford, D., Curtis, A., *et al.* (1996) *Am. J. Hum. Genet.* **59,** 16–22.
5. Trottier, Y., Lutz, Y., Stevanin, G., Imbert, G., Devys, D., Cancel, G., Sandou, F., Weber, C., David, G., Tora, L., *et al.* (1995) *Nature (London)* **378,** 403–406.
6. Perutz, M. F., Johnston, T., Suzuki, M. & Finch, J. T. (1994) *Proc. Natl. Acad. Sci USA* **91,** 5355–5358.
7. Perutz, M. F. (1996) *Curr. Opin. Struct. Biol.* **6,** 848–858.
8. Scherzinger, E., Lurz, R., Turmaine, M., Mangiarini, L., Hollenbach, B., Hasenbank, R., Bates, G. P., Davies, S. W., Lehrach, H. & Wanker, E. E. (1997) *Cell* **90,** 549–558.
9. Davies, S. W., Turmaine, M., Cozens, B. A., DiFiglia, M., Sharp, A. H., Ross, C. A., Scherzinger, E., Wanker, E. E., Mangiarini, L. & Bates, G. P. (1997) *Cell* **90,** 537–548.
10. Schmitz, S. K. (1990) *An Introduction to Dynamic Light Scattering by Macromolecules* (Academic, New York).
11. Chu, B. (1991) *Dynamic Light Scattering* (Academic, New York).
12. Brown, W., ed. (1993) *Dynamic Light Scattering: The Method and Some Applications* (Oxford Science, London).
13. Lomakin, A., Chung, D., Benedek, G., Kirschner, D. & Teplow, D. (1996) *Proc. Natl. Acad. Sci. USA* **93,** 1125–1129.
14. Tomski, S. & Murphy, R. M. (1992) *Arch. Biochem. Biophys.* **294,** 630–638.
15. Shen, C.-L., Fitzgerald, M. C. & Murphy, R. M. (1994) *Biophys. J.* **67,** 1238–1246.
16. Shen, C.-L., Grayson, L. S., Merchant, F. & Murphy, R. M. (1993) *Biophys. J.* **65,** 2383–2395.
17. Lomakin, A., Teplow, D. B., Kirschner, D. A. & Benedek, G. B. (1997) *Proc. Natl. Acad. Sci. USA* **94,** 7942–7947.
18. Pusey, P. N. & Tough, R. J. A. (1985) in *Dynamic Light Scattering*, ed. Pecora, R. (Plenum, New York), pp. 85–179.
19. Koppel, D. E. (1972) *J. Chem. Phys.* **57,** 4814–4820.
20. Wills, P. R. & Georgalis, Y. (1981) *J. Phys. Chem.* **85,** 3978–3984.
21. Doi, M. & Edwards, S. F. (1995) *The Theory of Polymer Dynamics* (Oxford Science, London).
22. Fujime, S. & Maeda, T. (1985) *Macromolecules* **18,** 191–195.
23. Maeda, T. & Fujime, S. (1985) *Macromolecules* **18,** 2430–2437.
24. Maeda, T. (1991) *Macromolecules* **24,** 2740–2747.
25. Aragon, S. R. & Pecora, R. (1985) *Macromolecules* **18,** 1868–1875.
26. Tracy, M. A. & Pecora, R. (1992) *Annu. Rev. Phys. Chem.* **43,** 525–557.
27. Harper, J. D. & Lansbury, P. T., Jr. (1997) *Annu. Rev. Biochem.* **66,** 385–407.
28. Caputo, C. B., Fraser, P. E., Sobel, I. E. & Krischner, D. A. (1992) *Arch. Biochem. Biophys.* **292,** 199–205.